Rupture of molecular thin films observed in atomic force microscopy. II. Experiment

Simona Loi,[1] Gexiao Sun,[2] Volker Franz,[1] and Hans-Jürgen Butt[2,*]
[1]*Physikalische Chemie, Universität Siegen, 57068 Siegen, Germany*
[2]*Max-Planck-Institute for Polymer Research, Ackermannweg 10, 55128 Mainz, Germany*
(Received 17 April 2002; published 5 September 2002)

In atomic force microscope studies of thin films often a defined jump of the tip through the film is observed once a certain threshold force has been exceeded. In particular, on lipid bilayers this is regularly observed. In a previous paper [H.-J. Butt and V. Franz, Phys. Rev. E **66**, 031601 (2002)] we presented two complementary models to describe film rupture. The aim of this study was to verify these models. Experiments were done with solid supported bilayers consisting of dioleoyloxypropyl-trimethylammonium chloride (DOTAP) and dioleoylphosphatidylserine (DOPS) in aqueous solutions and with propanol. Both models describe experimental results adequately. In particular, a narrow distribution of yield forces and an increase of the mean yield force with increasing loading rate is correctly predicted. For the lipid bilayers spreading pressures of roughly 20 mN/m (DOTAP) and 5 mN/m (DOPS) were measured. Line tensions for the edge of a lipid bilayer ranged between 3 (DOTAP) and 6 pN (DOPS).

DOI: 10.1103/PhysRevE.66.031602 PACS number(s): 68.37.−d, 68.15.+e, 68.47.Pe, 64.60.Qb

I. INTRODUCTION

The atomic force microscope (AFM) has become an important tool to analyze thin films. Most studies are devoted to image their surface topography to obtain information about the film structure under nonvacuum conditions with high resolution. During recent years, more and more groups have measured force-versus-distance curves, briefly called ''force curves,'' to obtain additional information. Force curves can, for instance, provide information about the mechanical properties of thin films. This paper deals with a typical feature of force curves: in AFM studies of molecular thin films often a defined jump of the tip through the film is observed once a certain threshold force has been exceeded. Such tip induced film ruptures have been observed on solid supported lipid bilayers and on surfactant layers. In addition, when studying confined liquids with the AFM often several jumps are observed which corresponds to squeezing layer after layer out of the gap between tip and substrate.

In a previous paper we proposed a theory on tip induced film rupture [1]. The aim of this paper is to verify our theory with experimental results measured in different systems. Our concern is not only to extract microscopic parameters of the film but also in general a better understanding of rupture and failure on the nanometer scale. The first part of our theory on tip induced film rupture is relatively general. It was only assumed that the tip has to overcome an activation energy before the film ruptures. We obtain a universal relation between the force dependence of the activation energy ΔU and the force dependence of the loading rate ν (the ''loading rate'' is the approaching velocity of the base of the cantilever),

$$\Delta U(F_0) = -k_B T \ln\left(\frac{0.693K}{A}\frac{d\nu}{dF_0}\right). \tag{1}$$

The idea is to measure $\nu(F_0)$, calculate $d\nu/dF_0$, and then use Eq. (1) to determine $\Delta U(F_0)$. Here, F_0 is the mean applied force when the film ruptures, k_B and T are the Boltzmann's constant and the temperature, K is the spring constant of the cantilever. The factor A is the frequency at which the tip ''attempts'' to penetrate the film.

In addition to the general approach, we propose two specific models to calculate the activation energy: one is a continuum nucleation theory, the other is a model which explicitly takes the molecular nature of the film into account. With these models we calculate how the probability to find the tip on top of the film (no rupture) P depends on the applied force F, the loading rate, etc.

In the continuum nucleation model we consider a molecular thin, homogeneous film confined between the solid substrate and the solid surface of the tip. The film is supposed to by laterally in a liquid state, but vertically its structure is well defined. Then we obtain.

$$\ln P(F) = -\frac{A}{K\nu}\int_{F_S}^{F}\exp\left(-\frac{2\pi^2\Gamma^2 R}{F'-F_S}\right)dF', \tag{2}$$

with $F_S = 2\pi RS$. Here, $S = \gamma_{TL} + \gamma_{SL} - \gamma_{TF} - \gamma_{SF}$ is the effective spreading pressure. To describe the notation we assume that the experiment is performed in a liquid state. This is, for instance, the case if a lipid bilayer is studied in an aqueous medium. Then γ_{TF} is the energy of the tip-film interface, γ_{TL} is the energy of the tip-liquid interface, γ_{SF} is the energy of the substrate-film interface, and γ_{SL} is the energy of the substrate-liquid interface; all values are given in energy per unit area. The line tension Γ represents the free energy associated with the unsaturated bonds of the molecules at the periphery of the hole. R is the radius of curvature of the tip.

In the molecular model each molecule in the film has certain binding sites, which are energetically favorable positions. To jump from a binding site to an adjacent free binding site a potential energy barrier has to be overcome. In the absence of the tip, adjacent binding sites are energetically

*Author to whom correspondence should be addressed. FAX: +49-271-7403198; email address: butt@chemie.uni-siegen.de

equivalent. When the tip is pressed onto the film, a pressure gradient is applied which increases the energy of the molecules. It becomes energetically favorable for the molecules to jump to the side and form a hole in the center of the tip. Once a certain critical number of molecules have jumped out of the contact area, the pressure upon the remaining molecules in the gap is so high that they also jump out of the gap. The film ruptures and the tip penetrates. This model predicts a probability distribution

$$\ln P = -\frac{k_0 F_T}{K\nu}(e^{F/F_T}-1), \tag{3}$$

with

$$F_T \equiv \frac{4\pi h R k_B T}{V}. \tag{4}$$

Here, k_0 is a rate constant for the spontaneous (without a tip) formation of holes in units of Hz. The activation volume V is the volume of the critical number of molecules. We assumed that the activation barrier between neighboring binding sites is symmetric. Thus the parameter α of the previous paper [1] was set to 0.5. For the mean yield force, we obtain

$$F_0 = F_T \ln\left(\frac{0.693K}{k_0 F_T}\nu + 1\right). \tag{5}$$

It is proportional to the logarithm of the loading rate.

To test the theory, we performed experiments with two types of solid supported lipid bilayers. Both were formed by spontaneous vesicle fusion on mica. In addition, the layered structure of 1-propanol was investigated. Propanol was demonstrated to form a layered structure between the planar mica and the tip surface, once the gap has closed to roughly 3 nm [2]. Three distinct force maxima are observed, which we believe to be correlated with the removal of three layers of alcohols out of the closing gap. For the different lipid layers and the alcohol many force curves were taken at different loading rates. The results were compared to theoretical predictions.

II. MATERIALS AND METHODS

Measurements were carried out with a commercial AFM (NanoScope 3, Multimode, Veeco Instruments, Santa Barbara, CA) and silicon nitride cantilevers (Veeco Instruments, CA, length 200 or 100 μm, width 40 μm, estimated thickness 0.6 μm). We calibrated the AFM scanner in the vertical direction as described by Jaschke and Butt [3]. Cantilever spring constants were individually determined by moving them against a calibrated reference cantilever [4]. Spring constants ranged from 0.07 to 0.45 N/m.

In addition to untreated tips, some tips were coated with 2 nm chromium and 10 nm gold by thermal evaporation. Care was taken to avoid evaporating too much gold on the tips since in this case the cantilevers bend. After evaporation, the tips were immediately immersed in a 1 m*M* 11-mercapto-1-undecanol (97%, Aldrich) solution in ethanol (per analysi grade, 99.8%, Merck) for at least 15 h. The radius of the tip curvature was measured by imaging a silicon grating TGT01 (MikroMasch, Oelsnitz, Germany) that is much sharper than the tip itself (radius of curvature less than 10 nm). In this way, the topology of the tip was determined. Then the tip shape was fitted to a circle. The radius of the tip curvature was estimated by making an average of several radii of circles in different directions. Tip radii of untreated silicon nitride tips were between 26 and 51 nm. For thiolated tips the radii ranged from 48 to 94 nm.

The shape of force curves taken with thiolated tips was the same as with untreated silicon nitride tips. Usually, however, results obtained on lipid bilayers were more reproducible. This poor reproducibility of untreated silicon nitride tips involves several aspects: force curves measured with bare silicon nitride tips sometimes displayed shorter jump-in distances. Second, bare silicon nitride tips sometimes showed two breakthroughs, which was not observed using thiolated tips. Third, F_0-vs-ν curves obtained with different silicon nitride tips varied considerably more than F_0-vs-ν curves measured with thiolated tips. A possible reason is that thiol monolayers on gold form a chemically more homogeneous surface than the naturally oxidized silicon nitride surface.

All chemicals were of analytical grade and were used without further treatment. We purchased DOTAP from Aldrich, Steinheim, Germany. Providers of the other materials were Merck, Darmstadt, Germany (chloroform, KCl, KOH), Fluka, Neu-Ulm, Germany (NaCl), and Plano GmbH, Wetzlar, Germany (Muscovite mica). We used 1-propanol (per analysi grade) from Merck, Darmstadt, Germany, without further purification. It was dried over molecular sieves (LAB, 0.3 nm, Merck) under dry argon for at least 24 h.

Lipid vesicles for adsorption on mica were prepared as follows: DOTAP or DOPS was first dissolved in chloroform. Then the solvent was evaporated under a constant stream of N_2. A buffer solution of 150 m*M* NaCl and 5 m*M* KH_2PO_4 (that was titrated to *p*H 7.4 with KOH) was added to produce a 5 mg/ml suspension which was thoroughly sonicated (G112SP1T sonicator, Laboratory Supplies Co., Hicksville, NY) until the suspension became opalescent. Mica was freshly cleaved and mounted onto the AFM scanner. Immediately after cleavage, a drop of buffer solution was placed on the mica. Then, the AFM head with the liquid cell, O ring, and tip was mounted. Subsequently, 50 μl of the vesicle solution were pipetted into the cell. After 30 min adsorption time the cell was rinsed with approximately 1 ml buffer solution to remove vesicles that did not adsorb to the mica substrate. The measurement was started 20 min later.

In an alcohol experiment the alcohol was filled onto mica immediately after cleavage. Then, the AFM head with the liquid cell, O-ring, and tip was mounted and the liquid cell was completely filled with alcohol. After waiting at least 30 min the experiments were started.

In a force measurement, the sample is moved up and down by applying a voltage to the piezoelectric translator onto which the sample is mounted, while measuring the cantilever deflection. The result of such a measurement is a graph, which shows the cantilever deflection Δz_c versus the height position of the piezo. From this, a force-versus-

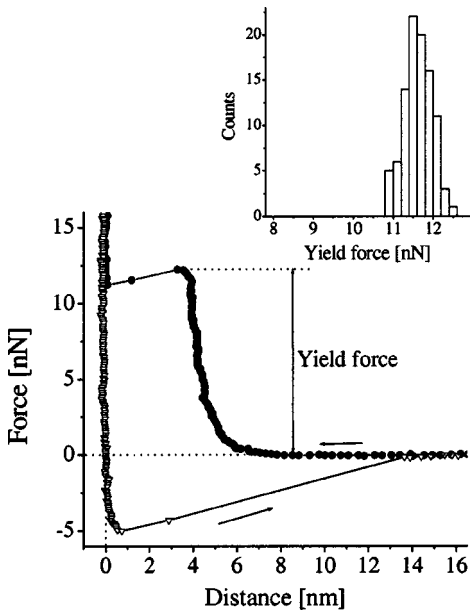

FIG. 1. A typical force curve measured on a lipid bilayer of dioleoyloxypropyl-trimethylammonium chloride (DOTAP) in aqueous electrolyte (150 mM NaCl, 5 mM KH_2PO_4, *p*H 7.4) taken at a loading rate $\nu = 2\ \mu$m/s. Approaching (●) and retracting (▽) parts are shown. The tip was coated with gold and a monolayer of hydroxy undecanethiol (tip radius $R = 67$ nm, spring constant of cantilever $K = 0.40$ N/m). As an inset the histogram of yield forces is shown.

distance curve is calculated by multiplying the cantilever deflection with its spring constant K to obtain the force, $F = K\Delta z_c$, and subtracting the cantilever deflection from the height position to obtain the distance. In this paper only the force is relevant because the theory is only concerned with the strength of the yield force. The distance dependency of force curves is only important to identify the film rupture and the jump of the tip. From the approach part of force curves we obtain the force at which the breakthrough occurs—the yield force. Yield forces are collected for 50–400 measurements at different approaching velocities. The results for each velocity are plotted in a histogram.

Experimentally determined histograms of yield forces and F_0-vs-ν curves were fitted with the continuum nucleation model, Eq. (2), and with the molecular model, Eqs. (3) and (5). In the first case it was not a true fit but parameters were adjusted by eye.

III. RESULTS AND DISCUSSION

A. Yield forces on lipid bilayers

Figure 1 shows a typical force curve taken on a DOTAP bilayer. Far away from the surface no force is acting on the tip. Decreasing the distance between tip and sample below roughly 6 nm leads to a sharp increase of the repulsive force. Finally an instability occurs, the tip breaks through, and the lipid film ruptures.

In Fig. 2 a histogram of yield forces extracted from 400 force curves measured at a loading rate of 2 μm/s is shown.

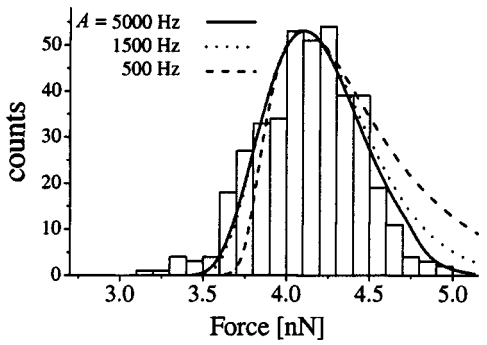

FIG. 2. Histogram of yield forces measured on a DOTAP bilayer with an untreated silicon nitride tip ($R = 49$ nm, $K = 0.09$ N/m, $\nu = 2\ \mu$m/s) in aqueous electrolyte. The lines in the histogram were calculated with the continuum nucleation model, Eq. (2), using three different frequency factors A. For each frequency factor the two remaining parameters, the line tension Γ and spreading pressure S were varied until an optimal fit was achieved. Results in this particular case were: $\Gamma = 3.5\times10^{-12}$ N/m, $S = 0.0095$ N/m for $A = 5$ kHz; $\Gamma = 2.0\times10^{-12}$ N/m, $S = 0.0110$ N/m for $A = 1.5$ kHz; $\Gamma = 1.0\times10^{-12}$ N/m, $S = 0.0120$ N/m for $A = 0.5$ kHz.

Such histograms were recorded for yield forces at different loading rates. Their maxima and widths for three different experiments with DOTAP are shown in Fig. 3. For all measurements the mean yield force increased linearly with logarithmically increasing loading rates. Straight lines are curves fitted with

$$F_0 = a + b \ln \nu. \tag{6}$$

The constants a and b were determined from the fit. All numbers given were obtained with loading rates in units of μm/s.

B. Force dependence of the activation energy

To obtain more information about the activation energy we apply Eq. (1). Therefore $d\nu/dF_0$ could be determined from results such as those shown in Fig. 3. Then $\Delta U(F_0)$ could be calculated. In the case of lipid bilayers, however, a more precise analysis is possible. Assuming that the mean yield forces increase linearly with the logarithm of the loading rate according to Eq. (6) it follows that $d\nu/dF_0 = \ln 10\ v/b$. Inserting this into Eq. (1) leads to

$$\Delta U(F_0) = -k_B T \ln\left(\frac{1.60K}{Ab}\nu\right)$$

$$= k_B T\left[2.30\frac{a-F_0}{b} - \ln\left(\frac{1.60K}{Ab}\right)\right]. \tag{7}$$

A general result is that the activation energy decreases linearly with increasing applied force.

As an example we consider a typical experiment done with a thiolated tip on a DOTAP bilayer. The parameters in this particular experiment were $K = 0.36$ N/m and $R = 86$ nm. By fitting measured F_0-vs-ν curves with Eq. (6) we obtained $a = 12.7$ nN and $b = 1.39$ nN. Taking $A = 5$ kHz to be the resonance frequency of the cantilever in aqueous

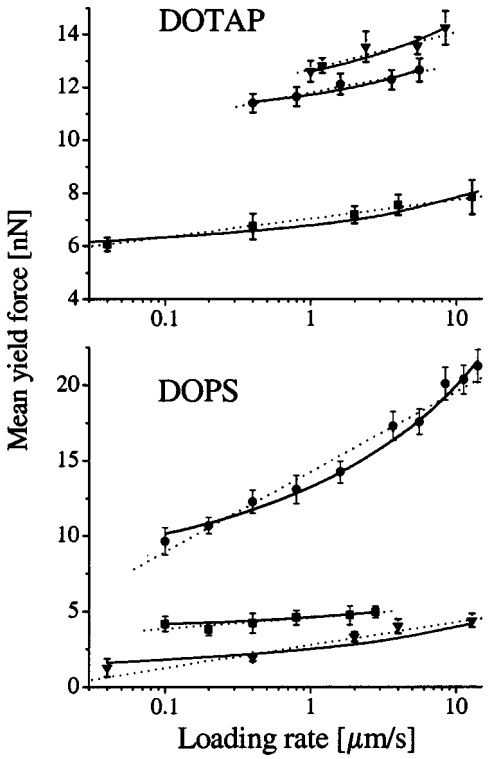

FIG. 3. Dependence of the mean yield forces on the loading rate as measured on DOTAP (top) and DOPS (bottom) bilayers in typical experiments. Error bars indicate the half width of peaks in the corresponding histograms. DOTAP: ▼, $R=86$ nm, $K=0.36$ N/m, OH-gold coated tip; ●, $R=67$ nm, $K=0.40$ N/m, OH-gold coated tip; ■, $R=49$ nm, $K=0.09$ N/m, bare silicon nitride tip. DOPS: ▼, $R=26$ nm, $K=0.09$ N/m, bare silicon nitride tip; ●, $R=82$ nm, $K=0.45$ N/m, OH-gold coated tip; ■, $R=69$ nm, $K=0.07$ N/m, OH-gold coated tip. The continuous lines were calculated with the nucleation model. Dotted lines were obtained with the molecular model, Eq. (5).

medium (see below) we get $\Delta U=k_BT(9.7-1.7F_0)$, where F_0 has to be given in nN. As an average we get $\Delta U=k_BT(10-2.2F_0)$ for DOTAP and $\Delta U=k_BT(3.5-1.8F_0)$ for DOPS and thiolated tips. The respective numbers in kJ/mol are $\Delta U=25-5.4F_0$ and $\Delta U=9-4.4F_0$; again F_0 has to be inserted in nN. For $F_0=0$ this is of the same order of magnitude as effective activation energies determined for the diffusion of lipid molecules in phospholipid bilayers which are 20–50 kJ/mol [5–8].

C. Fitting experimental results with the continuum nucleation model

As a first step we check whether the typical histograms can be fitted with the continuum nucleation model. In the continuum nucleation model we have three parameters: the frequency factor A, the line tension Γ, and the spreading pressure S. The frequency factor cannot exceed the resonance frequency of the cantilever, which in water is in the order of 5 kHz. Therefore we start the fitting procedure by choosing a certain value of A and then let Γ and S vary until the best agreement is reached using Eq. (2). It turned out that A should be chosen as high as possible. With increasing A the peak becomes more narrow and symmetric. The smaller A, the broader and the more asymmetric the force peak becomes. In the example shown in Fig. 2, choosing $A=5$ kHz to be equal to the resonance frequency gave the best results. An optimal fit was achieved with $\Gamma=3.5\times10^{-12}$ N/m and $S=9.5$ mN/m. With $A=1.5$ kHz still reasonable agreement was achieved using $\Gamma=2.0\times10^{-12}$ N/m and $S=11.0$ mN/m. For $A=0.5$ kHz the calculated peak was too asymmetric and we reject this solution. We conclude that the frequency factor should be chosen to be equal to the resonance frequency. Even if A was wrong by a factor of three the resulting line tension and the spreading pressure varied only by less than a factor two.

In addition to the histogram, the model should be able to reproduce the dependence of the mean yield force on the loading rate (Fig. 3). The graph $F_0(\nu)$ can in fact be used to get more precise values for the spreading pressure and the line tension. Experimental curves could be fitted with the nucleation model and relatively well defined values for S and Γ were obtained. The errors of S and Γ due to the fit are less than 30%.

Fitting mean yield force-versus-loading rate (F_0-vs-ν) curves with the continuum nucleation model does not lead to a linear increase with $\ln\nu$ but the curves increase more steeply with increasing loading rate. In some experiments this tendency was indeed observed. The difference is, however, not significant.

D. Comparing DOTAP and DOPS

Qualitatively, the same behavior was observed on DOPS bilayers as on DOTAP bilayers. Defined yield forces, which were distributed in a narrow peak around a mean yield force; the mean yield force increased with the loading rate (Fig. 3 bottom). Quantitatively, DOPS and DOTAP bilayers lead to different values of the spreading pressure and the line tension (Table I). For DOPS we determined a relatively low spreading pressure and a high line tension (mean values $S=0.0058$ N/m, $\Gamma=6.0$ pN). For DOTAP the spreading pressure was higher and the line tension was lower ($S=0.017$ N/m, $\Gamma=2.4$ pN). This indicates that for DOTAP the interaction with the substrate is stronger than for DOPS while the interaction between the lipid molecules is lower. This experimental finding agrees with what is expected: the positively charged trimethylammonium head group of DOTAP is known to strongly adsorb to the negatively charged mica while the adsorption of the negatively charged DOPS is weaker.

The line tensions determined are in the same range as line tensions of phospholipid monolayers and bilayers reported in the literature. A theoretical estimation for bilayers leads to $\Gamma\approx10$ pN [9,10]. Analyzing pore formation in bilayers resulted in typical line tensions of 6–30 pN [11–13]. Electroporation and electromechanical experiments indicate a line tension for bilayers of $\Gamma=2-37$ pN [14–16]. Different lipid domains in monolayers show typical line tensions of 0.9–1.6 pN [17,18]. Only one value determined from AFM images of patches of bilayers which resulted in Γ

TABLE I. Summary of experimental results obtained with bare silicon nitride tips (SiN) and gold-hydroxy undecanethiol coated tips (OH). Results obtained with the continuum nucleation model are characterized by the spreading pressure S (in 10^{-3} N m) and the line tension Γ (in 10^{-12} N) setting $A=5$ kHz. In the molecular model the relevant parameters are the rate of spontaneous hole formation k_0 and the activation volume V. To calculate the activation volume with Eq. (4) a thickness of 4.0 and 0.95 nm was used for the lipid bilayers and propanol, respectively. For each combination of tip and medium three or more experiments were done, except for DOPS with untreated silicon nitride tips. For this reason, no error is given in this case.

Sample	Tip	S (mN m)	Γ (pN)	$\ln k_0$ (k_0 in Hz)	V (N m^3)
DOTAP	SiN	13.3 ± 2.9	2.2 ± 1.2	$-(6.5\pm1.8)$	11.7 ± 2.3
DOTAP	OH	22.6 ± 2.4	2.8 ± 0.8	$-(7.5\pm1.1)$	7.6 ± 1.3
DOPS	SiN	3.3	7.9	0.1	2.0
DOPS	OH	7.4 ± 1.3	5.4 ± 2.4	$-(2.3\pm1.2)$	7.9 ± 3.5
Propanol 1, first	OH	6.9 ± 1.9	2.4 ± 0.6	$-(4.4\pm1.3)$	5.1×1.3
Propanol 1, second	OH	0.55 ± 0.20	0.03 ± 0.01	0.7 ± 0.8	44 ± 8

$\approx10^{-6}$ pN is much lower than line tensions deduced from AFM induced film rupture [22].

The spreading pressure is relevant for the vesicle adsorption to solid surfaces. Values reported in the literature are, however, scarce. From the kinetics of spreading Rädler *et al.* estimate a gain in free energy per unit area for the adsorption of lipid bilayers of 0.2 mN/m [19].

E. Fitting experimental results with the molecular model

Using the molecular model histograms (Fig. 4) and F_0-vs-ν curves (Fig. 3) could be fitted. In particular, the linear increase of the mean yield force with loading rate is predicted by Eq. (5) of the model. Only two parameters, the activation volume and the rate constant k_0, have to be determined. This can be done in a unique way from experimental F_0-vs-ν curves. The experimental results are fitted by Eq. (6). Then the thermal force F_T and k_0 are obtained from

$$F_T = b \ln e = 0.434b, \qquad k_0 = 1.596 \frac{K}{b} 10^{-(a/b+6)} \frac{m}{s}. \tag{8}$$

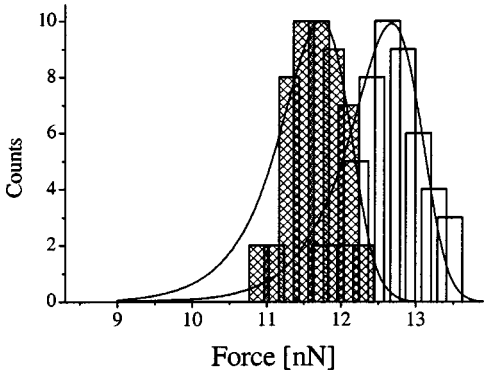

FIG. 4. Histogram of yield forces measured on a DOTAP bilayer with a gold and hydroxythiol coated tip ($R=67$ nm, $K=0.4$ N/m) at loading rates of $\nu=0.8$ μm/s (left peak) and 5.6 μm/s (right peak) in aqueous electrolyte. The lines in the histogram were calculated with the molecular model, Eq. (4), using $F_T=0.45$ nN and $k_0=2.5\times10^{-9}$ Hz.

From F_T the activation volume can be calculated with Eq. (4). The factor 10^6 occurs because in F_0-vs-ν plots the loading rate is given in μm/s.

Activation volumes determined were roughly 10 nm^3 for DOTAP and 5 nm^3 DOPS; this difference is not yet significant. This activation volume contains $n\approx4-7$ lipid molecules. The rate of spontaneous hole formation was much lower on DOTAP than on DOPS bilayers. The geometric mean values were $k_0=1.3\times10^{-7}$ Hz for DOTAP and $k_0=1.9\times10^{-2}$ Hz for DOPS which probably reflect the stronger binding of DOTAP to mica and the higher mobility of DOPS on mica.

These rates can be compared to jump frequencies of lipid molecules in solid supported membranes measured with different techniques such as fluorescence recovery after photobleaching or by nuclear magnetic resonance [5,8,20,21]. In both techniques the lateral diffusion coefficient D is determined. This can be converted to a jump frequency of single lipid molecules between adjacent binding sites ν_0 according to $D=\frac{1}{4}\nu_0{}^2$ [7]. Here, λ is the distance between neighboring binding sites. Typical values for solid supported phospholipid bilayers are $D\approx7\times10^{-12}$ m^2/s. With $\lambda=0.7$ nm jump frequencies of 10^8 Hz are obtained. This is much higher than the values we obtained for k_0. This, however, is not surprising because to form a hole large enough to initate tip penetration and film rupture, typically ten molecules have to jump at the same time.

F. Propanol

When measuring force curves in 1-propanol (Fig. 5) three repulsive, equidistant maxima were observed. This indicates that propanol assumes a layered structure in the closing gap between tip and substrate surface. We analyzed the first and second layer. As ''first layer'' we denote the one which is squeezed out at a distance of ≈0.95 nm. A histogram of yield forces clearly shows two peaks corresponding to the two layers. Mean yield forces of both layers increased with increasing loading rate (Fig. 6), as predicted by theory.

Parameters determined for the first layer of propanol were of the same order of magnitude as those obtained for the lipids—despite the fact that the layer is four times thinner

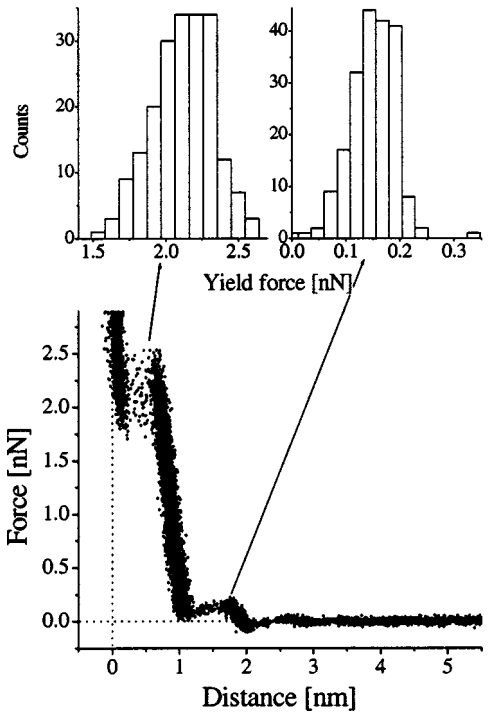

FIG. 5. Bottom: force-vs-distance curve obtained in propanol on mica. The AFM tip ($R=48$ nm, $K=0.22$ N/m, $\nu=1.1$ μm/s) was coated with gold and a monolayer of hydroxy undecanethiol. The force curve is a superposition of ≈ 70 individual approaching force curves. Top: histograms of yield forces for the first (left) and second (right) layers.

than the lipid bilayer. When interpreting results obtained with the molecular model it is instructive to estimate the critical number of molecules in the activation volume n. With $n=\rho V/m$ (ρ is the density of propanol and m is the mass of a molecule) this number is $n=41$. It is significantly higher than for lipid bilayers. This could also explain why the rate k_0 is not much higher for the small alcohol molecules than for the lipids: to form a hole large enough to initiate film rupture many more molecules have to jump out of the contact area.

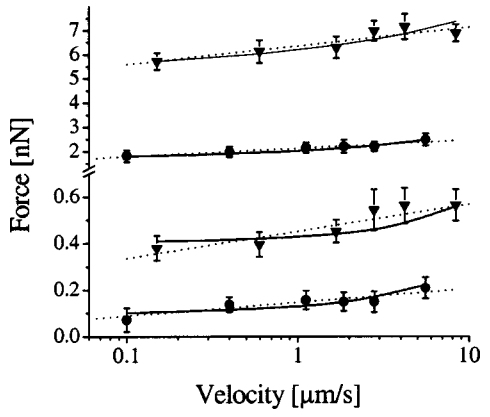

FIG. 6. Mean yield forces vs the loading rate measured in propanol for two experiments (●, $R=48$ nm, $K=0.22$ N/m, and ▼, $R=86$ nm, $K=0.18$ N/m). Results for the first (high force) and second layer (low force) are shown. The AFM tips were coated with gold and a monolayer of hydroxy undecanethiol.

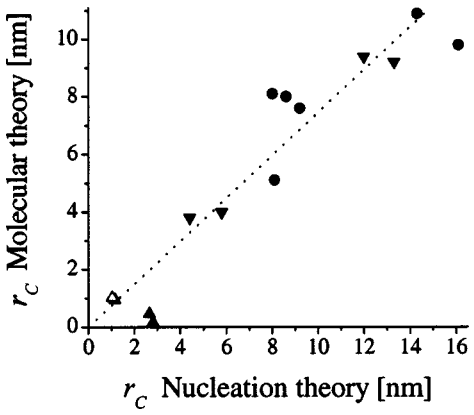

FIG. 7. Correlation between the critical radii r_C of the molecular model and the continuum nucleation model. For the nucleation model a yield force according to a loading rate of 1 μm/s was inserted. As a layer thickness we used $h=4$ nm for the lipid bilayers and 0.95 nm for propanol. ●, DOTAP; ▼, DOPS; △, propanol first layer; ▲, propanol second layer.

G. Comparison between the continuum nucleation and the molecular models

Based on the experimental results it is not possible to decide which model is better or to reject one model entirely. Within the experimental errors both models agree with the results. What are the major differences between the two models and where are the similarities? First, over a wide range of loading rates and applied forces both models do not exclude each other. They highlight different features of the film from different points of view. One such feature is the size of the hole, which is large enough to initiate film rupture. In the molecular model the radius of this hole can simply be calculated from the activation volume according to

$$r_C=\sqrt{\frac{V}{\pi h}}. \tag{9}$$

In nucleation theory this critical radius is given by [1]

$$r_C=\frac{2\pi R\Gamma}{F-2\pi RS}. \tag{10}$$

Taking results obtained at a loading rate of 1 μm/s, a typical value in AFM force experiments, we find a remarkable agreement between the two models (Fig. 7). For all measurements the ratio between the critical radius obtained with the molecular model and the critical radius determined with the nucleation model was between 0.61 and 1.01. There was only one exception: the second layer in propanol. For the second layer of propanol this ratio was between 6 and 20. This might indicate that for this layer the treatment as a film using our theory is not adequate. At least it behaves fundamentally different from the first layer and from the lipid bilayers.

There are, however, also significant differences between the nucleation and the molecular model. First, the nucleation model predicts a certain threshold force $F_S = 2\pi RS$. The mean yield force has to be higher than this minimal value. Second, the mean yield force increases more than $\propto \ln \nu$. Thus, at least in principle it should be possible to distinguish between the two models for a specific film if one could expand the accessible range of loading rates.

IV. CONCLUSIONS

The activation energy for the rupture of lipid bilayers or alcohol films under the influence of an AFM tip decreases linearly with the applied force. Extrapolating to zero force, the activation energies agree with values reported in the literature. Two complementary models for the rupture process, the continuum nucleation model and the molecular model, describe film rupture adequately. Microscopic parameters derived are reasonable with respect to values determined with other methods and with respect to results obtained for different materials. Using the kinetic theory, force curves measured with the AFM on molecular thin films can quantitatively be evaluated.

ACKNOWLEDGMENT

We thank the Deutsche Forschungsgemeinschaft for financial support, Grant Nos. Bu 701/14 (S.L.), Bu 701/21 (G.S.), and Bu 701/19 (V.F.).

[1] H.-J. Butt and V. Franz, Phys. Rev. E **66**, 031601 (2002).
[2] V. Franz and H.-J. Butt, J. Phys. Chem. B **106**, 1703 (2002).
[3] M. Jaschke and H.-J. Butt, Rev. Sci. Instrum. **66**, 1258 (1995).
[4] M. Preuss and H.-J. Butt, Langmuir **14**, 3164 (1998).
[5] L. K. Tamm and E. Kalb, *Molecular Luminescence Spectroscopy*, edited by S. G. Schulman (Wiley, New York, 1993), Vol. 77, p. 253.
[6] P. Karakatsanis and T. M. Bayerl, Phys. Rev. E **54**, 1785 (1996).
[7] H.-J. Galla, W. Hartmann, U. Theilen, and E. Sackmann, J. Membr. Biol. **48**, 215 (1979).
[8] R. Merkel, E. Sackmann, and E. Evans, J. Phys. (France) **50**, 1535 (1989).
[9] W. Helfrich, Phys. Lett. **50**, 115 (1974).
[10] J. D. Litster, Phys. Lett. **53**, 193 (1975).
[11] C. Taupin, M. Dvolaitzky, and C. Sauterey, Biochemistry **14**, 4771 (1975).
[12] D. V. Zhelev and D. Needham, Biochim. Biophys. Acta **1147**, 89 (1993).
[13] J. D. Moroz and P. Nelson, Biophys. J. **72**, 2211 (1997).
[14] I. Genco, A. Gliozzi, A. Relini, M. Robello, and E. Scalas, Biochim. Biophys. Acta **1149**, 10 (1993).
[15] W. Harbich and W. Helfrich, Z. Naturforsch. A **34a**, 1063 (1979).
[16] V. F. Pastushenko, Y. A. Chizmadzhev, and V. B. Arakelyan, J. Electroanal. Chem. **104**, 53 (1979).
[17] D. J. Benvegnu and H. M. McConnell, J. Phys. Chem. **96**, 6820 (1992).
[18] P. Steffen, P. Heinig, S. Wurlitzer, Z. Khattari, and T. M. Fischer, J. Phys. Chem. **115**, 994 (2001).
[19] J. Rädler, H. Strey, and E. Sackmann, Langmuir **11**, 4539 (1995).
[20] C. Dolainsky, M. Unger, M. Bloom, and T. M. Bayerl, Phys. Rev. E **51**, 4743 (1995).
[21] J. Kusba, L. Li, I. Gryczynski, G. Piszczek, M. Johnson, and J. R. Lakowicz, Biophys. J. **82**, 1358 (2002).
[22] A. S. Muresau and K. Y. C. Lee, Langmuir **105**, 852 (2001).